ChemComm

Dynamic Article Links▶

COMMUNICATION

Liquid Crystalline Macrocyclic Azacalix[4]pyridine and Its Complexes with Zinc Ion: Conformational Change from Saddle to Flattened Shape†

Shi-Xin Fa,[a] Xiao-Fang Chen,[b] Shuang Yang,[b] De-Xian Wang,[a] Liang Zhao,[c] Er-Qiang Chen,*[b] and Mei-Xiang Wang*[c]

Substituted with four 3,4,5-tris(alkoxy)benzyl mini-dendrons, azacalix[4]pyridine (1) with saddle-shaped core is the first liquid crystal (LC) of heteracalixaromatics. Conformational
10 **regulation of azacalix[4]pyridine by complexing with zinc ion leads to significant change of LC properties.**

As a new type of macrocyclic hosts in supramolecular chemistry, heteracalixaromatics, the heteroatom bridged calix(het)arenes which assemble various aromatic rings by different heteroatoms,
15 have been attracting considerable interest.[1] Particularly, since the bridging heteroatoms can adopt different electronic configurations and form various degrees of conjugation with their neighboring aromatic rings, conformational structures and cavity sizes of heteracalixaromatics are self-regulated, rendering
20 macrocycles versatile in molecular recognition.[2] For example, as shown in Fig. 1, tetramethylazacalix[4]pyridine can change its conformation remarkably from saddle-shaped 1,3-alternate with an approximate C_{2v} symmetry to that with the dramatic planarization of the macrocyclic backbone with a S_4 symmetry
25 upon the formation of coordination complexes with transition metals.[3] Such a conformational regulation of macrocycle is of particular interest in supramolecular chemistry. Moreover, it may influence the self-assembly in condensed state. To manipulate the molecular packing and processibility, considering their
30 intrinsically anisotropic molecular shape, one effective strategy is introducing liquid crystal (LC) properties to heteracalixaromatics. Although macrocycle-derived mesogens have gained great attention[4] since the first example of macrocyclic LC was reported in 1980,[5] no direct evidence of the effect of variation of
35 macrocyclic conformations on the LC phase behaviours of macrocyclic mesogens has been reported so far. Here, we study N-[3,4,5-tris(tetradecyloxy)benzyl]-bridged calix[4]pyridine (1) and its complexes with zinc salts. The significant change of phase behaviour from complex monotropic to enantiotropic columnar
40 LC phase (Col) demonstrates that the conformational variation of the azacalix[4]pyridine core plays an important role.

Synthetic routes of the azacalix[4]pyridine derivative **1** and the zinc complexes are shown in Scheme 1. Based on our previous study,[6] the parent NH-bridged calix[4]pyridine macrocycle **4** was
45 easily synthesized in 37% yield from the Pd-catalyzed reaction of 2,6-bis(allylamino)pyridine **2** with N_2,N_6-bis(6-bromopyridin-2-yl)-N_2,N_6-diallylpyridine-2,6-diamine **3** followed by exhaustive *N*-deallylation reaction. With the aid of NaH as a strong base,

compound **4** underwent nucleophilic substitution reaction with
50 benzyl bromide **5** to afford desired product **1** in 54% yield. Refluxing **1** with zinc salts in a mixture of dichloromethane and methanol (1:1) led to the formation of **1**·ZnA$_2$ complexes in good to excellent yields. Structures of **1** and its zinc complexes were confirmed by spectroscopic data and elemental analyses. It is
55 worth to mention that **1** and each of its complexes give a single set of proton and carbon signals in ^{1}H and ^{13}C NMR spectra (see ESI†), respectively, in agreement with the highly symmetric conformational structures illustrated in Fig. 1 and Scheme 1.

Fig. 1 Dramatic change of conformational structure of 1,3-
65 alternate azacalix[4]pyridine from saddle-shaped to flattened one upon interaction with zinc ion.
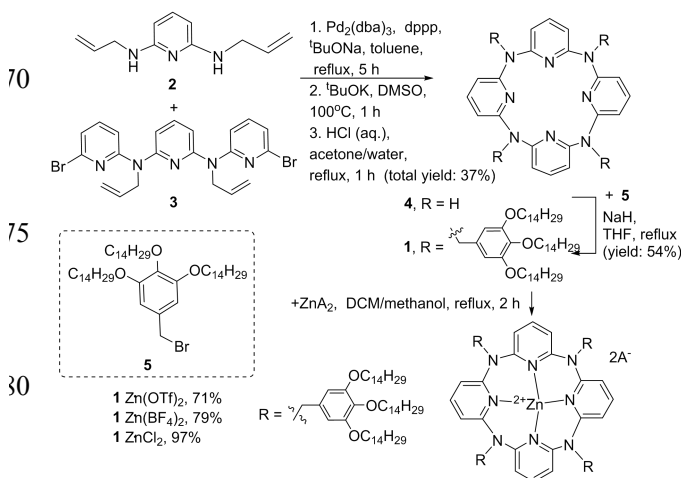
Scheme 1. Synthesis of azacalix[4]pyridine derivative **1** and its
85 zinc complexes.

The thermal properties of compound **1** and its complexes
1·ZnA$_2$ were first investigated by using differential scanning calorimetry (DSC) and polarizing optical microscopy (POM).
90 The temperature and enthalpy of the transitions of the four samples are listed in Table 1.The phase transition behaviour of **1**

is in fact monotropic depending greatly on the DSC scan rate, whereas those of the prepared complexes are enantiotropic (see Fig. S1 and S4, ESI†). Fig. 2 shows the POM results. The texture featuring Col phase is obtained when isotropic **1** was slowly
5 cooled to 49 °C (Fig. 2a). However, while being kept at the same temperature, spherulites with Maltese cross extinction pattern could develop gradually from the LC phase, indicating the formation of a crystal (Cr) phase (Fig. 2b).[7] The Cr phase would melt only when the temperature was increased to *ca*. 70 °C, *ca*.
10 20 °C higher than the LC isotropic temperature of **1**. Different from the parent macrocycle **1**, **1**·ZnCl₂ and **1**·Zn(BF₄)₂ could present the texture of Col at around 100 °C upon cooling the samples from isotropic state. When decreasing to ambient temperature, the birefringence became stronger. For **1**·Zn(OTf)₂,
15 no clear texture was observed during the whole cooling process.

Table 1. Thermodynamic data for **1** and its zinc-complexes.

	cooling[a,b,c]	heating[a,b,c]
1	iso 41.1 (-5.11) Col$_h$ -6.5 (-24.01) Col$_h^{or}$	Col$_h^{or}$ 5.4 (22.11) Col$_h$ 51.0 (5.77) iso
	iso 44.9 (-5.30) Col$_h$ -2.3 (-16.41) Col$_h^{or}$	Col$_h^{or}$ 7.2 (44.17) Col$_h$ 53.9 (25.61) Cr 70.2 (15.95) iso
1·ZnCl₂	iso 100.8 Col$_h$ 6.3 (-29.69) Col$_h^{or}$	Col$_h^{or}$ 14.3 (26.17) Col$_h$ 126.5 iso
1·Zn(BF₄)₂	iso 104.0 Col 13.3 (-23.41) Col^{or}	Col^{or} 20.4 (22.45) Col 121.7 iso
1·Zn(OTf)₂	X₁ -8.8 (-18.52) X₂[d]	X₂ -2.4 (24.62) X₁[d]

[a] Transition temperature in °C (in parentheses, transition enthalpy in J/g). [b] Data is read from the DSC cycles at a rate of 10 °C/min, while the second row of **1** is from the cycles at 0.5 °C/min. [c] Data only with temperature was obtained from the POM experiments. [d] X denotes the LC phase undetermined.

20
25
30
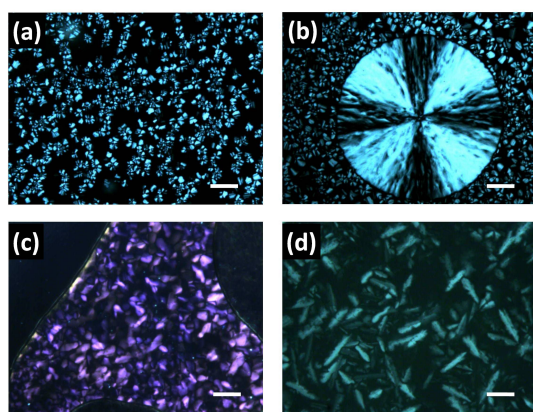
Fig. 2 POM textures of (a, b) **1**, (c) **1**·ZnCl₂, and (d) **1**·Zn(BF₄)₂ at 49 °C, 49 °C for 30 min, 101 °C, and 95 °C during cooling the samples from isotropic state, respectively. Scale bar: 100 μm.
35

The phase transitions of **1** and its complexes were further characterized by thermal one-dimensional (1D) X-ray diffraction (XRD) experiments. As shown in Fig. 3a, after pre-cooling the sample **1** rapidly to 0 °C from isotropic state, we observe four
40 sharp diffractions in the low-angle region with the scattering vector q ($q = 4\pi\sin\theta/\lambda$ with λ the X-ray wavelength and 2θ the scattering angle) being in the ratio of 1:√3:√4:√7 and a relatively

narrow diffraction at 0.42 nm in the high-angle region, which reveal the formation of the hexagonal columnar (Col$_h$) with sub-
45 nanometer order (Col$_h^{or}$) of **1**. Heating the sample to 40 °C leads to the disappearance of the high-angle diffraction at 0.42 nm and the retention of the first- and second- order diffractions with a 1:√3 q-ratio, indicating a Col$_h$. After heating to 50 °C, many diffractions in both low- and high-angle regions evolve,
50 suggesting the formation of a more stable Cr phase.
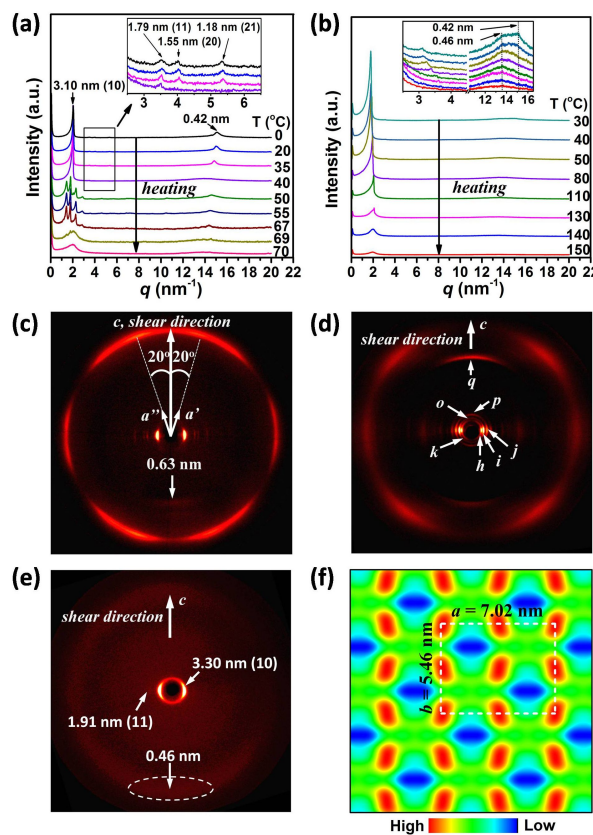
Fig. 3 (a, b) Set of 1D XRD patterns of (a) **1** and (b) **1**·ZnCl₂ recorded upon heating. (c, d, e) 2D XRD patterns of sheared (a, b) **1** and (d) **1**·ZnCl₂ recorded at room temperature. The X-ray beam was perpendicular to the shear direction. Sample **1** was sheared at 48 °C and (c) quenched to room temperature, (d) isothermal annealed at room temperature for 48 h and then at 60 °C for 60 h. (e) Sample **1**·ZnCl₂ was sheared at 80°C and quenched to room temperature. (f) Relative electron density map of **1** calculated based on the diffracted intensity of (hk0) shown in (d).

Fig. 3b depicts the thermal 1D XRD profiles of complex
90 **1**·ZnCl₂. At temperatures below 30 °C, it possesses three low-angle diffractions with the q-ratio of 1:√3:2 and a clear diffraction in the high-angle region at 0.42 nm, indicating a Col$_h^{or}$ phase. Similar with its parent compound **1**, increasing temperature leads the sample to enter the Col$_h$ phase. Note that this Col$_h$ phase can
95 exist in a rather wide temperature range up to 130 °C. However, complex **1**·ZnCl₂ cannot crystallize no matter what thermal treatment was applied. **1**·Zn(BF₄)₂ and **1**·Zn(OTf)₂ also have two transition processes shown by thermal XRD experiment, with the low temperature one corresponding to the melting of ordered
100 alkyl chains and the other of isotropization of LC phase at above

120 °C (see Fig. S5-S7, ESI†).

The experimental results illustrate that compound **1** possesses the Cr phase as the most stable one, which can develop from the metastable Col_h phase. For **1**·ZnA₂, enantiotropic LC behaviour appears, with the isotropic temperature much higher than that of **1**. To shed further light on their phase structures, we focused on the two-dimensional (2D) XRD results of the oriented samples prepared by mechanical shearing.

Fig. 3c shows the 2D XRD pattern of **1** recorded at room temperature. The (hk) diffractions of the Col_h^{or} are on the equator, indicating that the axes of columns are well aligned along the shear direction (the meridian). On the meridian, there is a pair of weak and diffuse arcs, whose corresponding *d*-spacing of 0.63 nm is comparable to the thickness of saddle-shaped core simulated (Fig. 4a, S2 and S3) and is also very close to that (*ca.* 0.62 nm) observed in the methylazacalix[4]pyridine single crystal.[3a] Therefore, this diffraction at 0.63 nm suggests that within a column the saddle-shaped azacalix[4]pyridine moieties stack parallel to each other. In the high-angle region, the two sets of diffractions with hexagonal symmetry at 0.42 nm reflect the ordered arrangement of the alkyl tails. This implies that the peripheral chains in Col_h^{or} of **1** form an ordered structure similar to α_H phase of alkane, whose *a*-axes (*a'* and *a''* in Fig. 3c) tilt 20° or -20° to the axis (*c*) of supramolecular columns. The results evidence the microphase segregation of the azacalix[4]pyridine cores and the peripheral chains in the supramolecular column.

Keeping the sheared sample of **1** at room temperature for a long time (e.g., several days) or annealing it at around 60 °C, the LC phase of **1** would turn into the Cr phase with the orientation perfectly retained, as shown in Fig. 3d. Supposing the diffractions on the equator to be (hk0), of which the three lowest-angle ones (*h*, *i*, *j* in Fig. 3d) are (110), (200) and (020), respectively, the lattice parameters for **1** are calculated to be: *a* = 7.02 nm, *b* = 5.46 nm, *γ* = 90°. Based on these parameters, all the diffractions on the equator can be well indexed (see Table S2, ESI†). Considering the axis of supramolecular columns perpendicular to the *ab* plane, the Cr structure of **1** is assigned to be orthorhombic. Fig. 3f provides a relative electron density map of **1** calculated based on the (hk0) diffractions, illustrating the molecular arrangement in the *ab* plane at *z* = 0. Each red area with the highest electron density represents the aromatic core of the macrocycle, while the surrounding areas are packed with aliphatic tails. Note that there are four supramolecular columns in each unit cell.[8] Accordingly, the cross section per column is estimated to be of *ca.* 9.6 nm², which is about 85% of that of Col_h phase for **1**. Considering the relative rigidity of azacalix[4]pyridine moiety, the shrinkage of the cross section implies the tilting of macrocyclic molecules with respect to the column axis.

On the meridian, the diffraction at 0.63 nm in Fig. 3c is replaced by a much stronger arc at 0.59 nm (indexed as arc *q*). This newly emerged diffraction shall be again resulted from the parallel stacking of the azacalix[4]pyridine cores which may slightly change its saddle shape after crystallization. Assuming 0.59 nm determined by 2D XRD to be the *c*-axis dimension of the Cr phase of **1**, each unit cell is calculated to contain four molecules based on the experimental density (0.96 g/cm³) and molar mass of the compound (3277). It seems in agreement with the packing scheme in 2D lattice shown in Fig. 3f. However,

three culminant diffractions (indexed by *o*, *p* and *k* in Fig. 3d) near the beam stop should not be overlooked. Note that the distance between *o* and the projection of *k* onto the meridian equals to that between spots *o* and *p*, and the projection of spot *k* onto the equator is just the (100). Therefore, the diffractions *o* (3.55 nm), *p* (2.68 nm), and *k* (4.25 nm) can be indexed as (003), (004), and (102), respectively. As a result, the diffraction on the meridian at 0.59 nm shall be (0018), identifying that the Cr structure of **1** possesses a large *c* parameter of 10.62 nm.

Such a long *c*-axis for **1** is worth addressing. The typical *d*-spacing between the two crystallized alkyl layers is about 0.42 nm,[9] which is mismatch with the thickness of macrocyclic core (*ca.* 0.63 nm).[3a] When **1** crystallizes, the macrocyclic core and aliphatic tails seek the manner of close packing simultaneously, and thus maximize on the whole the molecular interactions. One possible manner is slight rotation of molecules with respect to each other in the column, which will lead to a large *c* dimension.[4f-g,10] Note that there are strong diffraction arcs of 0.42 nm in the quadrants, which may reflect the molecules are tilted relative to the column axis with an angle of *ca.* 45° (Fig. 3d). In this case, we presume that the tilted **1** molecules are helically assembled in the column, giving an 18-fold helix (Fig. 4c). Such a delicate molecular arrangement in the Cr phase is somewhat difficult to be reached directly in the undercooled melt. However, the pre-order provided by the Col_h phase can facilitate the Cr formation.
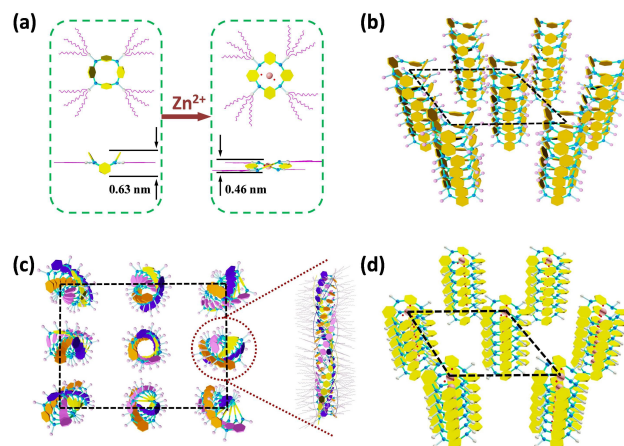
Fig. 4 (a) Schematic diagram of conformational variation of **1** by coordinating with zinc ion. Models of (b) the Col_h lattice on side view and (c) the slant helical column in the orthorhombic lattice(Cr) of **1**.(d) Col_h lattice on side view of **1**·ZnCl₂. For clarity, peripheral alkyl chains are not shown for Col phase and the four pyridine rings of the macrocyclic cores of Cr phase are drawn in different colours.

Shown by 2D XRD pattern in Fig. 3e for sheared **1**·ZnCl₂, the existence of supramolecular columns which are parallel to the shear direction can be confirmed as well. Albeit the high-angle scattering is weak, an intensity maximum at 0.46 nm on the meridian is observed. This scattering maximum is found also in the 1D XRD profiles of **1**·ZnCl₂ (Fig. 2b). Note that the estimated thickness of the coordinated azacalix[4]pyridine is about 0.45 nm.[3b] Therefore, the observed distance of 0.46 nm for **1**·ZnCl₂ can be referred to the average distance between two intra-

columnar adjacent zinc-azacalix[4]pyridine cores, which is remarkably reduced in comparison with that of 0.63 nm for **1** in Col$_h$ phase. Thusly, dramatic and stable conformational change of azacalix[4]pyridine by coordinating with zinc ions can persist well and consequently regulate the molecular packing in the mesomorphic phase (Fig. 4a and 4d).

We did not obtain the perfectly sheared samples of either **1**·Zn(BF$_4$)$_2$ or **1**·Zn(OTf)$_2$. Nevertheless, the scattering maximum at 0.46 nm in 1D XRD patterns can be clearly observed (Fig. S6 and S7, ESI†). Phase structures of these two complexes are not well solved since only one strong and sharp low-angle diffraction was detected. Likely, **1**·Zn(BF$_4$)$_2$ also forms supramolecular columns; however, the long-range 2D positional order of Col$_h$ at least partially loses. For **1**·Zn(OTf)$_2$, its birefringence was hard to be observed under POM, probably due to that the LC domains were smaller than the wavelength of visible light. These outcomes illustrate that the molecular packing of **1**·ZnA$_2$ are affected by the size of counter-anions. Albeit the much flatter azacalix[4]pyridine core resulted from complexing with zinc ion is helpful to the parallel molecular stacking to form supramolecular column, the use of large anions, which should be located surrounding the column centre to keep the electric neutrality, imposes a negative effect in stabilizing Col$_h$ phase.

In summary, we have designed and efficiently synthesized the first example of LC materials constructed by saddle-shaped macrocyclic azacalix[4]pyridine **1**. The phase transition pathway of **1** towards the lowest free energy is largely kinetically dependent. Compound **1** takes Col$_h$ phase as the precursor to form the Cr with helical and tilted molecular stacking. Coordinating **1** with zinc salts leads to conformational change of the macrocyclic core from saddle-shaped to the flattened one, resulting in a significant expansion of the LC range. However, the size of the counter-anions greatly affects the stability of the supramolecular column. With the small counter-anion such as Cl$^-$, the complex can well develop into Col$_h$ phase. An anisotropic ion-conductivity is therefore anticipated for the well orientated complexes, considering that the Col$_h$ phase can be readily aligned using external field such as mechanical shearing. Currently the corresponding research is undergoing in our laboratory, aiming to realize the functional materials based on heteracalixaromatics.

Notes and references

^{a}*Beijing National Laboratory for Molecular Sciences, CAS Key Laboratory of Molecular Recognition and Function, Institute of Chemistry, Chinese Academy of Sciences, Beijing 100190, China.*
^{b}*Beijing National Laboratory for Molecular Sciences, Key Laboratory of Polymer Chemistry and Physics at the Ministry of Education, College of Chemistry and Molecular Engineering, Peking University, Beijing 100871, China.*
E-mail: eqchen@pku.edu.cn
^{c}*Key Laboratory of Bioorganic Phosphorus Chemistry and Chemical Biology (Ministry of Education), Tsinghua University, Beijing 100084. China.*
E-mail: wangmx@mail.tsinghua.edu.cn

1   (a) M.-X. Wang, *Acc. Chem. Res.*, 2012, **45**, 182; (b) W. Maes and W. Dehaen, *Chem. Soc. Rev.*, 2008, **37**, 2393; (c) M.-X. Wang, *Chem. Commun.*, 2008, 4541.

2   (a) M.-X. Wang, X.-H. Zhang and Q.-Y.Zheng, *Angew.Chem., Int. Ed.*, 2004, **43**, 838; (b) M.-X. Wang and H.-B. Yang, *J. Am. Chem. Soc.*, 2004, **126**, 15412; (c) W. Van Rossom, M. Ovaere, L. Van Meervelt and W. Dehaen, *Org. Lett.*, 2009, **11**, 1681; (d) J.-T. Li, L.-X. Wang, L. Zhao, D.-X. Wang and M.-X. Wang, *J. Org. Chem.*, 2014, **79**, 2178.

3   (a) H.-Y. Gong, X.-H. Zhang, D.-X. Wang, H.-W. Ma, Q.-Y. Zheng and M.-X. Wang, *Chem. Eur. J.*, 2006, **12**, 9262; (b) Y. Miyazaki, T. Kanbare and T. Yamamoto, *Tetrahedron Lett.*, 2002, **43**, 7945; (c) H.-Y. Gong, Q.-Y. Zheng, X.-H. Zhang, D.-X. Wang and M.-X. Wang, *Org. Lett.*, 2006, **8**, 4895.

4   (a) S. H. Seo, T. V. Jones, H. Seyler, J. O. Peters, T. H. Kim, J.-Y. Chang and G. N. Tew, *J. Am. Chem. Soc.*, 2006, **128**, 9264; (b) H. Engelkamp, S. Middelbeek and R. J. M. Nolte, *Science*, 1999, **284**, 785; (c) M. Stępień, B. Donnio and J. L. Sessler, *Angew. Chem., Int. Ed.*, 2007, **46**, 1431; (d) C. Tschierske, *Top. Curr. Chem.*, 2012, **318**, 109; (e) B. Zhang, C.-H. Hsu, Z.-Q. Yu, S. Yang and E.-Q. Chen, *Chem. Commun.*, 2013, **49**, 8872; (f) V. Percec, M. R. Imam, M. Peterca, D. A. Wilson and P. A. Heiney, *J. Am. Chem. Soc.*, 2009, **131**, 1294; (g) C. Roche, H.-J. Sun, M. E. Predergast, P. Leowanawat, B. E. Partridge, P. A. Heiney, F. Araoka, R. Graf, H. W. Spiess, X.-B. Zeng, G. Ungar and V. Percec, *J. Am. Chem. Soc.*, 2014, **136**, 7169; (h) S. Kohmoto, Y. Someya, H. Masu, K. Yamaguchi and K. Kishikawa, *J. Org. Chem.*, 2006, **71**, 4509; (i) E. D. Baranoff, J. Voignier, T. Yasuda, V. Heitz, J. P. Sauvage and T. Kato, *Angew. Chem., Int. Ed.*, 2007, **46**, 4680; (j) I. Nierengarten, S. Guerra, M. Holler, J. F. Nierengarten and R. Deschenaux, *Chem. Commun.*, 2012, **48**, 8072; (k) K. Sato, Y. Itoh and T. Aida, *J. Am. Chem. Soc.*, 2011, **133**, 13767; (l) B. Xu and M. Swager, *J. Am. Chem. Soc.*, 1993, **115**, 1159.

5   J. W. Goodby, P. S. Robinson, B.-K. Teo and P. E. Cladis, *Mol. Cryst. Liq. Cryst.*, 1980, **56**, 303.

6   E.-X. Zhang, D.-X. Wang, Z.-T. Huang and M.-X. Wang, *J. Org. Chem.*, 2009, **74**, 8595.

7   W. Pisula, M. Kastler, D. Wasserfallen T. Pakula and K. Müllen, *J. Am. Chem. Soc.*, 2004, **126**, 8074.

8   (a) X.-H. Cheng, F. Liu, X.-B. Zeng, G. Ungar, J. Kain, S. Diele, M. Prehm and C.Tschierske, *J. Am. Chem. Soc.*, 2011, **133**, 7872; (b) B. Chen, U. Baumeister, G. Pelzl, M. K. Das, X.-B. Zeng, G. Ungar and C. Tschierske, *J. Am. Chem. Soc.*, 2005, **127**, 16578.

9   (a) H.-F. Shi, Y. Zhao, X. Dong, Y. Zhou, and D.-J. Wang, *Chem. Soc. Rev.*, 2013, **42**, 2075; (b) F. López-Carrasquero, A. Montserrat, A. Martínez de Ilarduya and S. Muñoz-Guerra, *Macromolecules*, 1995, **28**, 5535.

10 Z.-C. Liu, G.-L. Liu, Y.-L. Wu, D. Cao, J.-L. Sun, S. T. Schneebeli, M. S. Nassar, C. A. Mirkin and J. F. Stoddart, *J. Am. Chem. Soc.*, 2014, **136**, 16651.